Science, 2009, 324: 48–49
4 Rajesh B, Piotr Z. A class of non-precious metal composite catalysts for fuel cells. Nature, 2006, 443: 63–66
5 Bjorn W J, Orawan W J, Maria F, et al. High rates of oxygen reduction over a vapor phase-polymerized PEDOT electrode. Science, 2008, 321: 671–674
6 Ziegelbauer J M, Gullá A F, O'Laoire C, et al. Chalcogenide electrocatalysts for oxygen-depolarized aqueous hydrochloric acid electrolysis. Electrochim Acta, 2007, 52: 6282–6294
7 Bezerra C W B, Zhang L, Lee K C, et al. A review of Fe–N/C and Co–N/C catalysts for the oxygen reduction reaction. Electrochim Acta, 2008, 53: 4937–4951
8 Chen J, Zhang W M, Officer D, et al. A readily-prepared, convergent, oxygen reduction electrocatalyst. Chem Commun, 2007, 3353–3355
9 Lee K C, Zhang L, Lui H S, et al. Oxygen reduction reaction (ORR) catalyzed by carbon-supported cobalt polypyrrole (Co-PPy/C) electrocatalysts. Electrochim Acta, 2009, 54: 4704–4711
10 Lyth S M, Nabae Y, Moriya S, et al. Carbon nitride as a non precious catalyst for electrochemical oxygen reduction. J Phys Chem C, 2009, 113: 20148–20151
11 Biddinger E J, Deak D V, Ozkan U S. Nitrogen-containing carbon nanostructures as oxygen-reduction catalysts. Top Catal, 2009, 52: 1566–1574
12 Noto V D, Negro E. Development of nano-electrocatalysts based on carbon nitride supports for the ORR processes in PEM fuel cells. Electrochim Acta, 2010, 55: 7564–7574
13 Liu G, Li X G, Ganesan P, et al. Development of non-precious metal oxygen-reduction catalysts for PEM fuel cells based on N-doped ordered porous carbon. Appl Catal B-Environ, 2009, 93: 156–165
14 Gong K P, Du F, Xia Z H, et al. Nitrogen-doped carbon nanotube arrays with high electrocatalytic activity for oxygen reduction. Science, 2009, 323: 760–764
15 Tang Y F, Allen B L, Kauffman D R, et al. Electrocatalytic activity of nitrogen-doped carbon nanotube cups. J Am Chem Soc, 2009, 131: 13200–13201
16 Zhu C, Higgins D, Tao H S, et al. Highly active nitrogen-doped carbon nanotubes for oxygen reduction reaction in fuel cell applications. J Phys Chem C, 2009, 113: 21008–21013
17 Chen Z, Higgins D, Chen Z W, et al. Nitrogen doped carbon nanotubes and their impact on the oxygen reduction reaction in fuel cells. Carbon, 2010, 48: 3057–3065
18 Xiong W, Du F, Liu Y, et al. 3-D carbon nanotube structures used as high performance catalyst for oxygen reduction reaction. J Am Chem Soc, 2010, 132: 15839–15841
19 Yu D S, Zhang Q, Dai L M. Highly efficient metal-free growth of nitrogen-doped single-walled carbon nanotubes on plasma-etched substrates for oxygen reduction. J Am Chem Soc, 2010, 132: 15127–15129
20 Lefèvre M, Proietti E, Jaouen F, et al. Iron-based catalysts with improved oxygen reduction activity in polymer electrolyte fuel cells. Science, 2009, 324: 71–74
21 Qin H Y, Liu Z X, Ye L Q, et al. The use of polypyrrole modified carbon-supported cobalt hydroxide as cathode and anode catalysts for the direct borohydride fuel cell. J Power Sources, 2009, 192: 385–390
22 Qin H Y, Lao S J, Liu Z X, et al. Effects of heat treatment on the structure, morphology and electrocatalytic activity of cobalt hydroxide electrocatalyst. Int J Hydrogen Energy, 2010, 35: 1872–1878
23 Yoo E J, Okata T, Akita T, et al. Enhanced electrocatalytic activity of Pt subnanoclusters on graphene nanosheet surface. Nano Lett, 2009, 9: 2255–2259
24 Seger B, Kamat P V. Electrocatalytically active graphene-platinum nanocomposites. Role of 2-D carbon support in PEM fuel cells. J Phys Chem C, 2009, 113: 7990–7995
25 Qu L T, Liu Y, Baek J B, et al. Nitrogen-doped graphene as efficient metal-free electrocatalyst for oxygen reduction in fuel cells. ACS Nano, 2010, 4: 1321–1326
26 Shao Y Y, Zhang S, Engelhard M H, et al. Nitrogen-doped graphene and its electrochemical applications. J Mater Chem, 2010, 20: 7491–7496
27 Jafri R I, Rajalakshmi N, Ramaprabhu S. Nitrogen doped graphene nanoplatelets as catalyst support for oxygen reduction reaction in proton exchange membrane fuel cell. J Mater Chem, 2010, 20: 7114–7117
28 Lee K R, Lee K U, Lee J W, et al. Electrochemical oxygen reduction on nitrogen doped graphene sheets in acid media. Electrochem Commun, 2010, 12: 1052–1055
29 Sun Y Q, Li C, Xu Y X, et al. Chemically converted graphene as substrate for immobilizing and enhancing the activity of a polymer-iccatalyst. Chem Commun, 2010, 46: 4740–4742
30 Wei D C, Liu Y Q, Wang Y, et al. Synthesis of N-doped graphene by chemical vapor deposition and its electrical properties. Nano Lett, 2009, 9: 1752–1758
31 Li X L, Wang H L, Robinson J T, et al. Simultaneous nitrogen doping and reduction of graphene oxide. J Am Chem Soc, 2009, 131: 15939–15944
32 Zhang K, Zhang L L, Zhao X S, et al. Graphene/polyaniline nanofiber composites as supercapacitor. Chem Mater, 2010, 22: 1392–1401
33 Cote L J, Kim F, Huang J X. Langmuir Blodgett assembly of graphite oxide single layers. J Am Chem Soc, 2009, 131: 1043–1049
34 Jiang X, Ma Y W, Li J J, et al. Self-assembly of reduced graphene oxide into three-dimensional architecture by divalent ion linkage. J Phys Chem C, 2010, 114: 22462–22465
35 Guo H L, Wang X F, Qian Q Y, et al. A green approach to the synthesis of graphene nanosheets. ACS Nano, 2009, 9: 2653–2659
36 Ma Y W, Jiang S J, Jian G Q, et al. CN_x nanofibers converted from polypyrrole nanowires as platinum support for methanol oxidation. Energy Environ Sci, 2009, 2: 224–229
37 Zhang X T, Zhang J, Song W H, et al. Controllable synthesis of conducting polypyrrole nanostructures. J Phys Chem B, 2006, 110: 1158–1165
38 Kudin K N, Ozbas B, Schniepp H C, et al. Raman spectra of graphite oxide and functionalized graphene sheets. Nano Lett, 2008, 8: 36–41
39 Choi H C, Song H J, Jung H, et al. Release of N_2 from the carbon nanotubes *via* high-temperature annealing. J Phys Chem B, 2005, 109: 1683–1688

Supporting Information

SI 1 Thermogravimetry measurement of PPy/rGO powder
SI 2 Electrochemical impedance spectroscopy of CN_x/graphene composite

The supporting information is available online at csb.scichina.com and www.springerlink.com. The supporting materials are published as submitted, without typesetting or editing. The responsibility for scientific accuracy and content remains entirely with the authors.

Supporting Information

SI 1 Thermogravimetry measurement of PPy/rGO powder

Thermogravimetry (TG) and the corresponding derivation TG (DTG) profiles of PPy/rGO powder shown in Figure S1 were recorded by a STA-499F3 thermal analyzer (NETZSCH) at a 4 °C/min heating rate in Ar from about 25 to 1000°C. The decomposition of PPy/rGO is roughly divided into two stage according to the appearance of two main peaks around 106 and 350°C in the DTG curve. The first stage with the weight loss about 6% in the range of 25–180°C should come from the primary desorption of water. In the second weigh loss stage above 180°C is the thermal degradation and subsequent carbonization of PPy/rGO. The weight loss at 800°C is ~40%, slightly smaller than that at 1000°C (~46%). Considering that the carbonization at lower temperature would produce carbon nitride with higher nitrogen content, we selected the 800°C as the highest carbonization temperature, also according to our previous study (Ref. [36] in the text).

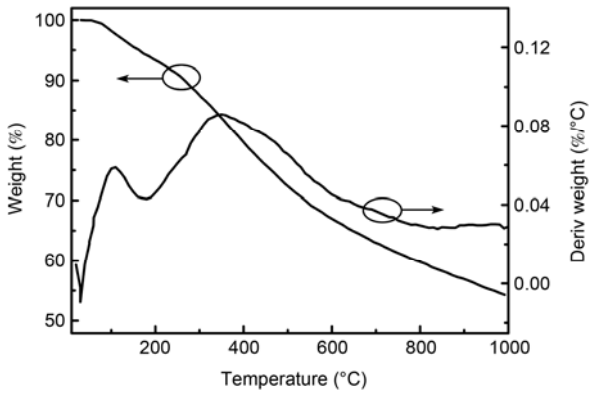

Figure S1 TG and DTG profiles of PPy/rGO composite at a heating rate of 4 °C/min.

SI 2 Electrochemical impedance spectroscopy of CN_x/graphene composite

Impedance measurements were performed for CN_x/graphene in 2 mol/L KOH aqueous electrolyte by the electrochemical impedance spectroscopy (EIS). EIS were measured with a frequency range of 0.01 Hz–100 kHz and the amplitude of modulation potential was 5 mV. The EIS data were analyzed using Nyquist plots as shown in Figure S2. These plots do not show semicircle regions, probably due to the low faradaic resistances of CN_x/graphene. From the x intercept, it's obtained that the equivalent series resistances of CN_x/G-600 and CN_x/G-800 are about 0.65 and 0.92 Ω, respectively. CN_x/G-800 has a smaller resistance than CN_x/G-600 probably due to the former carbonized at a higher temperature. The Warburg resistance, i.e., the 45° sloped portion of the Nyquist plots of CN_x/G-600 and CN_x/G-800 are very short, indicating that interfacial charge-transfer resistance among CN_x/graphene is significantly low, because of the high conductivity.

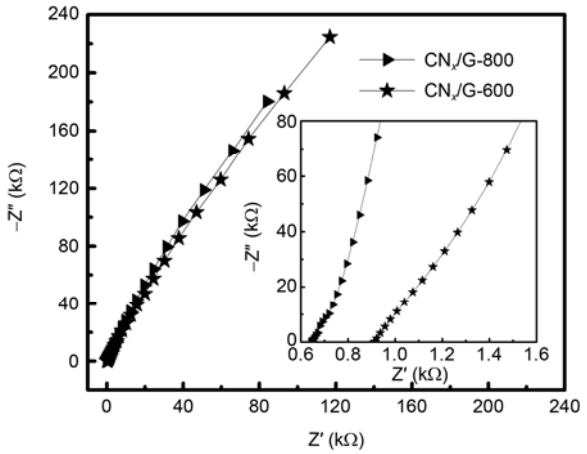

Figure S2 Nyquist plots of CN_x/G-600 and CN_x/G-800 composites. Inset shows the magnified high-frequency regions.